

## 21

### Membrane Emulsification: Principles and Applications

*Lidietta Giorno, Giorgio De Luca, Alberto Figoli,  
Emma Piacentini, and Enrico Drioli*

#### 21.1

##### Introduction

Emulsions and suspensions are colloidal dispersions of two or more immiscible phases in which one phase (disperse or internal phase) is dispersed as droplets or particles into another phase (continuous or dispersant phase). Therefore, various types of colloidal systems can be obtained. For example, oil/water and water/oil single emulsions can be prepared, as well as so-called multiple emulsions, which involve the preliminary emulsification of two phases (e.g., w/o or o/w), followed by secondary emulsification into a third phase leading to a three-phase mixture, such as w/o/w or o/w/o. Suspensions where a solid phase is dispersed into a liquid phase can also be obtained. In this case, solid particles can be (i) microspheres, for example, spherical particles composed of various natural and synthetic materials with diameters in the micrometer range: solid lipid microspheres, albumin microspheres, polymer microspheres; and (ii) capsules, for example, small, coated particles loaded with a solid, a liquid, a solid–liquid dispersion or solid–gas dispersion. Aerosols, where the internal phase is constituted by a solid or a liquid phase dispersed in air as a continuous phase, represent another type of colloidal system.

In emulsions and suspensions, disperse phase dimensions may vary from the molecular state to the coarse (visible) dispersion. They are commonly encountered in various productions. The average droplet/microcapsules size distribution is a key feature since they determine emulsions/suspensions properties for the intended uses and stability. For large-scale emulsion production, the most commonly employed methods are based on techniques aiming at establishing a turbulent regime in the fluid mixtures. These turbulent flows cannot be controlled or generated uniformly. The consequences are that the control of the droplet sizes is difficult and wide size distributions are commonly obtained, therefore the energy is used inefficiently in these technologies. In addition, the process scale-up is extremely difficult. The use of the ultrasonic bath yields better results with respects to the

mentioned procedures, however, the control of the droplet dimension is still not optimal.

For these reasons, recently much attention has been put in alternative emulsification processes, such as the membrane emulsification (ME).

Membrane emulsification is an appropriate technology for production of single and multiple emulsions and suspension. It was proposed for the first time at the 1988 Autumn Conference of the Society of Chemical Engineering, Japan. Since then, the method has continued to attract attention in particular in Japan, but also in Europe [1–10].

In the early 1990s, Nakashima *et al.* [2] introduced membrane technology in emulsions preparation by a direct emulsification method, whereas, in the late 1990s, Suzuki *et al.* used premix membrane emulsification to obtain production rates higher than other membrane emulsification methods [11].

The fast progress in microengineering and semiconductor technology led at the development of microchannels, that Nakajima *et al.* applied in emulsification technology [12].

The distinguishing feature of membrane emulsification technique is that droplet size is controlled primarily by the choice of the membrane, its microchannel structure and few process parameters, which can be used to tune droplets and emulsion properties. Comparing to the conventional emulsification processes, the membrane emulsification permits a better control of droplet-size distribution to be obtained, low energy, and materials consumption, modular and easy scale-up. Nevertheless, productivity ( $\text{m}^3/\text{day}$ ) is much lower, and therefore the challenge in the future is the development of new membranes and modules to keep the known advantages and maximize productivity.

Considerable progress has been achieved in understanding the technology from the experimental point of view, with the establishment of many empirical correlations. On the other hand, their theoretical interpretation by means of reliable models is not accordingly advanced. The first model devoted to membrane emulsification, based on a torque balance, was proposed in 1998 by Peng and Williams [13], that is, ten years later the first experimental work was published, and still nowadays, a theoretical study aiming at a specific description of the premix membrane emulsification process is not available.

The nonsynergistic progress of the theoretical understanding with the experimental achievements, did not refrain the technology application at the productive scale. In particular, membrane emulsification was successfully applied for preparation of emulsions and capsules having a high degree of droplet-size uniformity, obtained with low mechanical stress input [14–16]. Therefore, the application of membrane emulsification extended to various fields, such as drug delivery, biomedicine, food, cosmetics, plastics, chemistry, and some of these applications are now being developed at the commercial level. Their scale vary from large plants in the food industry, to medium-scale use in the polymer industry, and to laboratory-bench scale in biomedicine.

In this chapter, the experimental and theoretical bases as well as the applications of the technology will be discussed.

## 21.2 Membrane Emulsification Basic Concepts

Emulsions and suspensions are key systems for advanced formulations in various industrial sectors. Membrane emulsification is a relatively new technology in which membranes are not used as selective barriers to separate substances but as microstructures to form droplets with regular dimensions, that is, uniform or controlled droplet-size distribution (Figure 21.1). Membrane emulsifications can be generally distinguished in (Figure 21.2): (i) direct membrane emulsification (DME), in which the disperse phase is directly fed through the membrane pores to obtain the droplets, and (ii) premix membrane emulsification, in which a coarse premixed emulsion is pressed through the membrane pores to reduce and to control the droplet sizes.

In general, in the direct membrane emulsification, the disperse phase is pressed through a microporous membrane and droplets are formed at the opening of the pore on the other side of the membrane, which is in contact with the continuous phase. Here, droplets that reach a critical dimension can detach either for *spontaneous deformation* or are *sheared by the continuous phase* flowing parallel to the surface. In the former case, the driving force for the droplet formation is the surface free-energy minimization, that is, the droplet is formed by spontaneous deformation tending to form a sphere. For example, in quiescent conditions the droplets are formed by means of this mechanism. In the latter case, the shearing stress generated by the continuous phase is the driving force of the droplet detachment. For example, in the crossflow membrane emulsification (CDME) and stirred membrane emulsification droplets are formed by this mechanism.

In the premix emulsification the basic mechanism for the droplet formation is different from the direct emulsification. In fact, in this case the predominant formation mechanism is the droplet disruption within the pore.

Both direct and premix emulsification can be obtained with a continuous phase flowing along the membrane surface (i.e., crossflow, stirring) (Figure 21.2(b)). However, it is important to distinguish between the droplet-formation mechanism and the macroscopic operation procedure. In other terms, often, in the literature, the

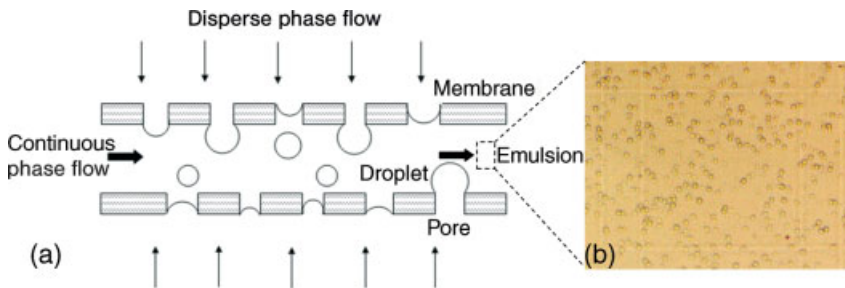


**Figure 21.1** Schematic representation (a) of membrane emulsification, where the membrane works as a high-throughput device to form droplets with regular dimensions; (b) photo of an o/w emulsion

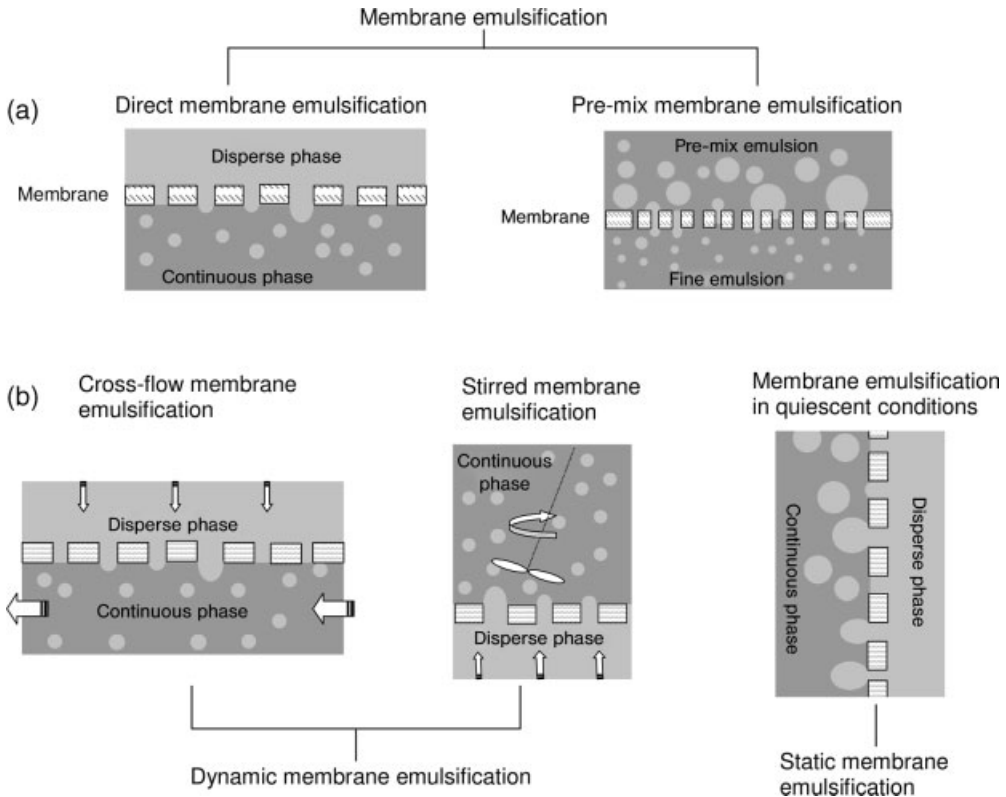


**Figure 21.2** Schematic drawing of membrane emulsification: (a) mechanisms (b) operation procedures.

'crossflow' term is used to indicate that the continuous phase is flowing along the surface, but this does not guarantee that the shear stress is the driving force for the droplet detachment, as long as the appropriate conditions are not verified.

The membrane emulsification can be considered as a case of microdevice emulsification process [17, 18] in which the porous membrane is used as micro-devices. Membrane emulsification carried out in quiescent conditions is also referred to as *static membrane emulsification*, while membrane emulsification carried out in moving conditions (either the membrane, i.e., rotating module, or the phase, i.e., crossflow) is also referred to as *dynamic membrane emulsification* (Figure 21.2(b)).

A peculiar advantage of membrane emulsification is that both droplet sizes and size distributions may be carefully and easily controlled by choosing suitable membranes and focusing on some fundamental process parameters reported below. Membrane emulsification is also an efficient process, since the energy-density requirement (energy input per cubic meter of emulsion produced, in the range of  $10^4$ – $10^6$  J m<sup>-3</sup>) is low with respect to other conventional mechanical methods ( $10^6$ – $10^8$  J m<sup>-3</sup>), especially for emulsions with droplet diameters smaller than 1 μm [1]. The lower energy density requirement also improves the quality and functionality

of labile emulsion ingredients, such as bioactive molecules. In fact, in conventional emulsification methods, the high shear rates and the resulting increase of the process temperature have negative effects on shear- or temperature-sensitive components. The shear stresses calculated for a membrane system are much less and it is possible to process shear-sensitive ingredients.

The droplet size, its dispersion and the droplet-formation time depend on several parameters: (i) *membrane parameters*, such as pore-size distribution, pore-border morphology, number of active pores, porosity, wetting property of the membrane surface, (ii) *operating parameters*, such as crossflow velocity (i.e., wall shear stress), transmembrane pressure and disperse-phase flow, temperature, as well as the membrane module used (tubular, flat, spiral-wound); and (iii) *phase parameters*, such as dynamic interfacial tension, viscosity and density of processed phases, emulsifier types, and concentration. Such quantities combine with different magnitudes, over the ranges of operating conditions, and many of them exhibit coupling effects<sup>4</sup>. Moreover, the production of monodisperse emulsions is essentially related to the size distribution of membrane pores and their relative spatial distribution on the membrane surface. It is worth noting that the geometry of the module in which the membrane is located is also an important parameter since it determines in conjugation to the crossflow velocity, the wall shear stress (Figure 21.3).

Droplet-size distribution and disperse-phase percentage determine the emulsion properties characterizing the final formulation for an intended use.

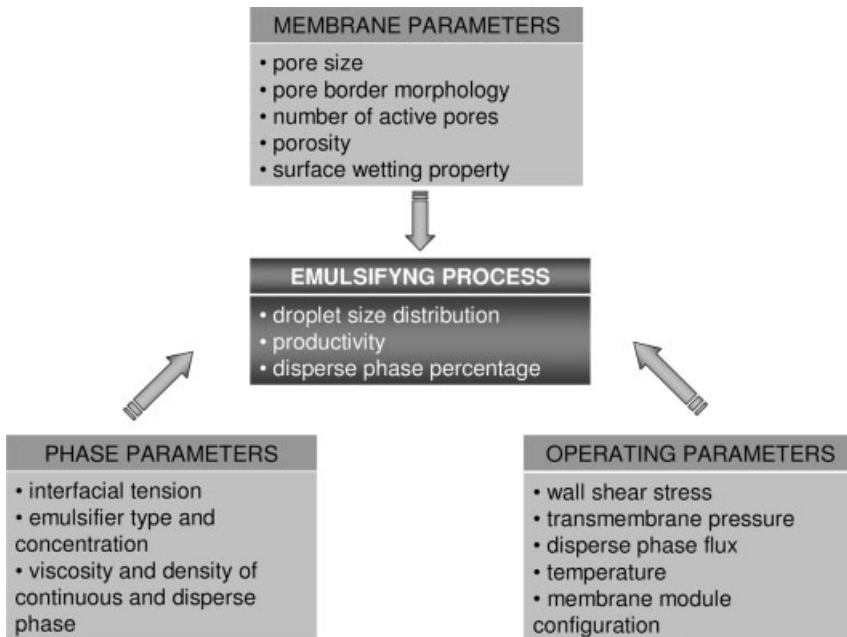


**Figure 21.3** Influence of parameters on droplet size and its formation during an emulsification process.

### 21.3

#### Experimental Bases of Membrane Emulsification

In this section, an analysis of the experimental observations and empirical correlations related to membrane emulsification processes will be illustrated. The theoretical bases that support these results and predict membrane emulsification performance will be discussed in the next section.

As previously anticipated, the appropriate choice of the membrane dictates the droplet properties. Membranes employed in emulsification processes are mainly of inorganic type (ceramic, glassy, metallic), but some examples of polymeric membranes have also been applied. Tables 21.1 and 21.2 summarize some of the most common membranes used in direct and premix membrane emulsification, respectively. Most of them have been originally developed for other membrane processes, such as microfiltration, and adapted in the emulsification technology. Nowadays, the growing interest towards membrane emulsification is also promoting research efforts in the design and development of membranes specifically devoted to membrane emulsification. Shirasu porous glassy (SPG) membranes were among the first membranes specifically developed for emulsion preparation. SPG membranes are characterized by interconnected micropores, a wide spectrum of available mean pore size (0.1–20  $\mu\text{m}$ ) and high porosity (50–60%). Micropore metallic membranes, developed by Micropore Technologies (United Kingdom), are characterized by cylindrical pores, uniform and in a regular array with a significant distance between each pore. They are available with pore diameters in the range of 5–20  $\mu\text{m}$  and exhibit very narrow pore-size distribution (Figure 21.4).

Membrane-wetting properties may be carefully considered in the membrane selection. In general, the membrane surface where the droplet is formed should not be wetted by the disperse phase. Therefore, a w/o emulsion is prepared using a hydrophobic membrane and an o/w emulsion is prepared using a hydrophilic membrane. On the other hand, w/o and o/w emulsions were successfully prepared using pretreated hydrophilic and hydrophobic membranes, respectively. The pretreatment basically consisted in absorbing the continuous phase on the membrane surface so that to render the membrane nonwetted by the disperse phase [14, 23, 25]. The presence of emulsifier in the disperse phase represents another strategy that permits the preparation of emulsions with a membrane wetted by the disperse phase.

The dispersion of droplet diameter mainly depends upon the membrane pore. In general, a linear relationship between membrane pore diameter ( $D_p$ ) and droplet diameter ( $D_d$ ) has been observed, especially for membranes with pore diameters larger than 0.1 micrometer. In these cases, linear coefficients varying between 2–10, depending on the operating conditions and emulsion composition, have been obtained [3, 23, 27]. Figure 21.5 summarizes the behavior of the mentioned relationships for different emulsion systems. In general, for a certain emulsion type and in comparable operating conditions, the lower the pore size the lower the droplet size.

Fluid-dynamic operating conditions, such as axial or angular velocity (i.e., shear stress that determines drag force value) and transmembrane pressure (that determines disperse-phase flux, for a given disperse-phase viscosity and membrane

Table 21.1 List of most common membranes used in direct membrane emulsification.

| Membrane material/wetting property                             | Membrane configuration | Pore geometry/porosity ( $\epsilon$ )                               | Pore diameter ( $\mu\text{m}$ ) | Membrane producer                          | Application           | Reference   |
|--|------------------------|---|---------------------------------|--|-----------------------|-------------|
| <b>Porous glass membrane</b><br>SPG/hydrophilic or hydrophobic | Tubular or disk        | Tortuous, interconnected cylindrical pore/ $50\% < \epsilon < 60\%$ | 0.1–20                          | SPG Technology Co., Ltd. (Japan)           | o/w, w/o emulsions    | [16, 19–21] |
| MPCG/hydrophilic   | Tubular or disk        | Cylindrical pore/ $50\% < \epsilon < 60\%$                          | 0.2–1.36;<br>10.2–16.2          | ISE Chemical Industries Co. Ltd (Japan)    | o/w and w/o emulsions | [21–23]     |
| Silica glass/hydrophobic                                       | Tubular                | Cylindrical pore/ $\epsilon = 61\%$                                 | 0.6                             | Lab-made                                   | w/o emulsions         | [24]        |
| <b>Ceramic membrane</b>  |                        |   |                                 |  |                       |             |
| Mullite ceramic/hydrophilic                                    | Disk                   | —   | 0.68                            | Lab-made                                   | w/o emulsions         | [25]        |
| Alumina/hydrophilic  | Tubular                | $\epsilon = 35\%$   | 0.1–0.8                         | Westfalia Separator Membraflow (Germany)   | o/w, w/o/w emulsions  | [5, 26–28]  |
|  |                        |   | 0.5–0.2                         | Société des Céramiques Techniques (France) | o/w emulsions         |             |
|  |                        |   | 0.5–0.8                         | Pall-Exekia (France)                       |                       |             |
| Zirconia/hydrophilic   | Tubular                | $\epsilon = 60\%$   | 0.1                             | Pall-Exekia (France)                       | o/w emulsions         | [27, 28]    |
|  |                        |   |                                 | Société des Céramiques Techniques (France) |                       |             |
| <b>Polymeric membrane</b>                                      |                        |   |                                 |  |                       |             |
| Polyamide/hydrophilic  | Hollow fiber           | —   | 10; 50 kDa (NMWCO) <sup>a</sup> | Forschstung Institut Berghof, (Germany)    | o/w emulsions         | [29]        |

(Continued)

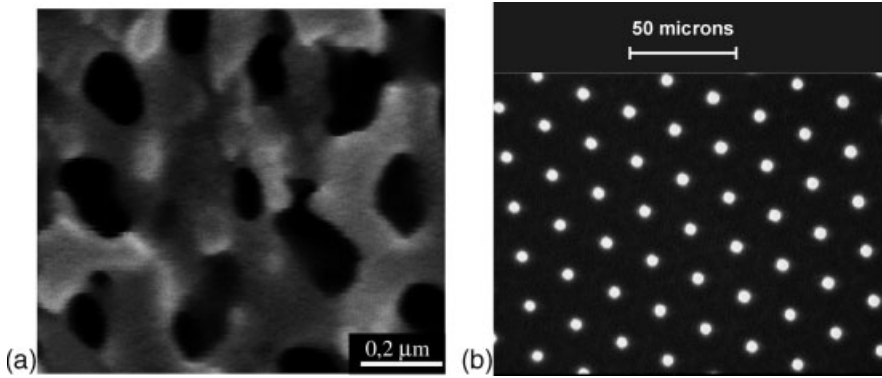
Table 21.1 (Continued)

| Membrane material/wetting property | Membrane configuration | Pore geometry/porosity ( $\epsilon$ ) | Pore diameter Membrane ( $\mu\text{m}$ ) producer | Application          | Reference |
|------------------------------------|------------------------|---------------------------------------|---|----------------------|-----------|
| PTFE/hydrophobic                   | Disk                   | $\epsilon = 79\%$                     | 0.5–50<br>Japan Goretex Co. (Japan)               |                      | [30]      |
| Polycarbonate/hydrophilic          | Disk                   | $5\% < \epsilon < 20\%$               | 10<br>ISOPORE, Nihon Millipore Co. (Japan)        |                      | [31]      |
| Cellulose acetate/hydrophilic      | Disk                   | —                                     | 0.2–03<br>Advantec Toyo (Japan)                   | w/o/w emulsions [32] |           |
| Polypropylene/hydrophobic          | Hollow fiber           | —                                     | 0.4<br>Wuppertal (Germany)                        | w/o emulsions [14]   |           |

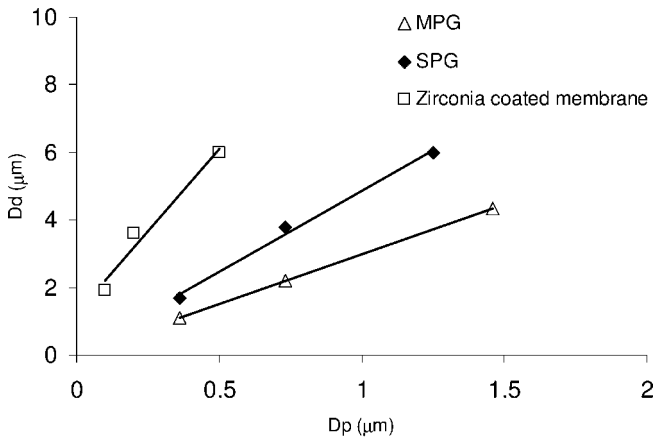
<sup>a</sup>Nominal molecular weight cutoff.

Table 21.2 List of most common membranes used in premix membrane emulsification.

| Membrane material                       | Membrane configuration | Operation mode     | Pore diameter ( $\mu\text{m}$ ) | Application     | Membrane producer                       | References |
|---|------------------------|--------------------|---------------------------------|-----------------|---|------------|
| Porous glass membrane<br>SPG            | Tubular                | Crossflow          | 2.7 and 4.2                     | o/w emulsions   | SPG Technology Co., Ltd.                | [11]       |
|   |                        | Deadend, multipass | 10.7                            | w/o/w emulsions | (Japan)                                 | [15]       |
| Ceramic membrane<br>Alumina/hydrophilic | Tubular                | Deadend, multipass | 3.2, 4, and 11                  | w/o/w emulsions | Lab-made                                | [33]       |
|   |                        | Deadend, multipass | 0.6, 0.8, and 3.0               | o/w emulsions   | Millipore corporation (United State)    | [34]       |
| Polymeric membrane<br>Polycarbonate     | flat                   | Deadend            | 0.2, 0.45, 0.8, and 3.0         | w/o/w emulsions | Advantec Toyo (Japan)                   | [35]       |
|   |                        | Deadend            | 0.8                             | o/w emulsions   | Whatman Intl. Ltd., Maidstone (England) | [36]       |



**Figure 21.4** Porous membranes developed for emulsification processes. (a) Shirasu porous glassy membrane (from SPG Technology Co., LTD, Japan), (b) metallic membrane (From Micropore Technologies, United Kingdom).



**Figure 21.5** Relationship between membrane pore diameter ( $D_p$ ) and droplet diameter ( $D_d$ ) (Data extrapolated from Refs. [3, 23, 27]).

properties), can be properly adapted to tune emulsion properties. The commonly observed behavior of shear stress and disperse-phase flux on  $D_d/D_p$  ratio is depicted in Figures 21.6 and 21.7, respectively. The droplet size decreases with increasing shear stress at the membrane surface and decreasing of the disperse-phase flux. However, the latter influence is less predominant and depends on the droplet-formation time, which in turn is strongly affected by the interfacial dynamical tension. If the droplet-formation time is larger than the complete adsorption of the emulsifier (equilibrium interfacial tension) the lower the influence of the disperse-phase flux. Therefore, in appropriate conditions and for emulsions with droplet size above a micrometer (1–50 micrometer, so-called macroemulsions), transmembrane

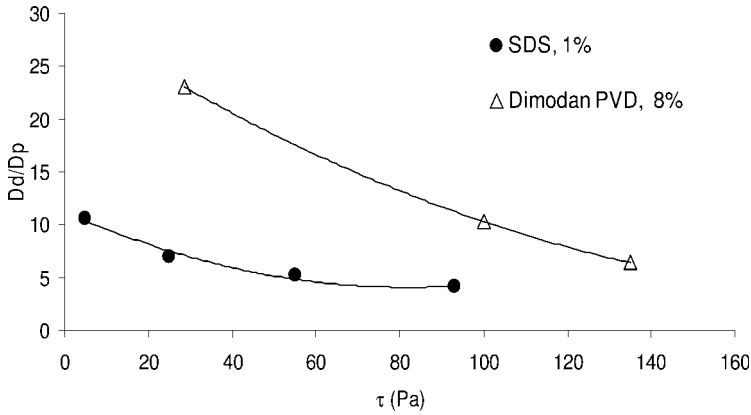


**Figure 21.6** Relationship between wall shear stress ( $\tau$ ) and  $D_d/D_p$  (Data extrapolated from Refs. [27, 28]).

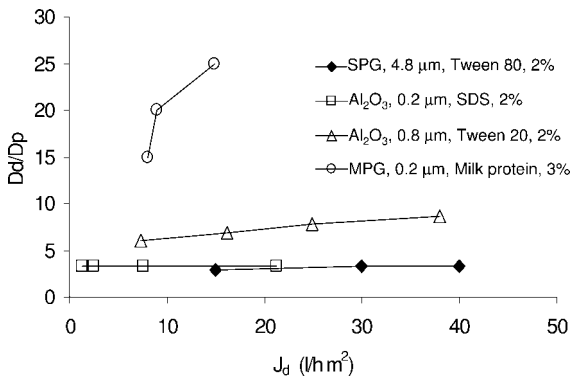


**Figure 21.7** Relationship between dispersed phase flux ( $J_d$ ) and  $D_d/D_p$  (Data extrapolated from Refs. [5, 16, 22, 26]).

pressure may influence the disperse-phase flux, but have little influence on changing the droplet size.

Dynamic interfacial tension, therefore the emulsifier used, and related adsorption kinetics influence the emulsification process. In general, the faster an emulsifier adsorbs to the newly formed interface, the lower the interfacial tension the smaller the droplet produced. Figure 21.8 shows a linear behavior between the  $D_d/D_p$  ratio and interfacial tension.

The axial velocity affects the droplet size by both influencing the surfactant mass transfer to the newly formed interface (that speeds up the reduction of the interfacial tension) and the drag force (that pulls droplets away from the pore mouth).

When production of submicrometer droplet size is aimed at, the continuous-phase shear stress and disperse-phase flux have to match the need for small droplet (i.e., high shear stress and low disperse-phase flux) with the need for a reliable system productivity (i.e., high disperse-phase flux).

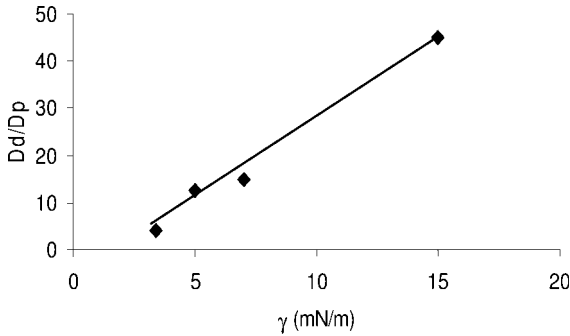


**Figure 21.8** Relationship between interfacial tension ( $\gamma$ ) and  $D_d/D_p$  (Data extrapolated from Ref. [26]).

The physical chemical properties of the phases can influence droplet formation as well as their stability in the bulk. For example, the viscosity of the continuous phase influences both the shear stress at the membrane wall and the adsorption kinetics of the emulsifier.

Concerning thermodynamically unstable emulsions, the creation of new interfaces from the disruption of the disperse phase increases the free energy of the system, which tends to return to the original two separate systems. Therefore, the use of emulsifier is necessary not only to reduce the interfacial tension, but also to avoid the coalescence and the formation of macroaggregates thanks to electrostatic repulsion between adsorbed emulsifier.

### 21.3.1

#### Post-Emulsification Steps for Microcapsules Production

In this paragraph, a description of postemulsification steps needed to complete the preparation of microcapsules is reported. Microencapsulation can be described as the formation of small, coated particles loaded with a solid, a liquid, a solid–liquid dispersion, gas or solid–gas dispersion (Figure 21.9). The concept of microencapsulation originated in the 1950s and provided the means by which ink formulations used in carbonless copy paper are packaged. This application has been most successful and has led to the development of other applications like the production of microcapsules for thermal printing, optical recording, photocopy toners,

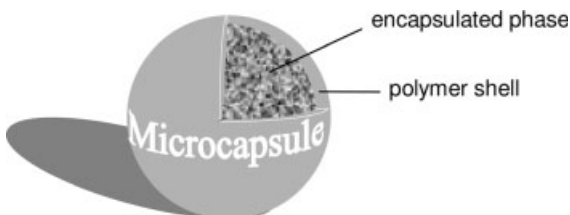


**Figure 21.9** Schematic drawing of a microcapsule.

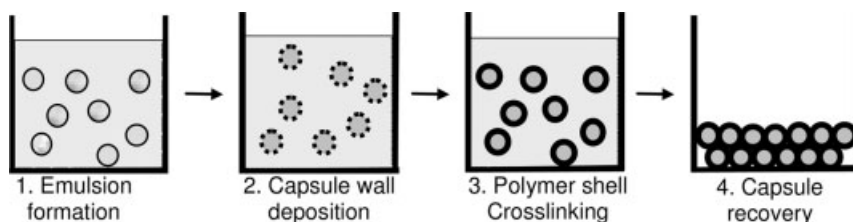


**Figure 21.10** Steps involved in the formation of microcapsules.

diazotizing, herbicides, animal repellents, pesticides, oral and injectable pharmaceuticals, cosmetics, food ingredients, adhesives, curing agents, and live-cell encapsulation [38].

The size of these capsules may range from 100 nm to about 1 mm. Therefore, they can be classified as nano-, micro- and macrocapsules, depending on their size. The first commercial microcapsules were made by Green with a process called complex coacervation [37]. Since then, other methods for preparing microcapsules have been developed of which some are based exclusively on physical phenomena. Some utilize polymerization reactions to produce a capsule shell. Others combine physical and chemical phenomena. But they all have three main steps in common. The steps of the microencapsulation preparation are schematically depicted in Figure 21.10. In the first step, a dispersion or emulsion has to be formed, followed by deposition of the material that forms the capsule wall (Figure 21.10, step 2). After solidification or crosslinking (step 3) of the droplets prepared, the capsules are isolated in the last step.

One of the major problems related to the capsule formation is capsule agglomeration. It involves the irreversible or largely irreversible sticking together of microcapsules that can occur during the encapsulation process and/or during the isolation step.

The microencapsulation process can be classified into two main categories (as defined by Thies [38] and reported in Table 21.3): (a) chemical process and (b) mechanical process.

**Table 21.3** List of encapsulation processes (After [38]).

| Chemical process                           | Mechanical process  |
|--|---|
| Complex coacervation                       | Spray drying  |
| Polymer/polymer incompatibility            | Spray chilling  |
| Interfacial polymerization in liquid media | Fluidized bed   |
| In situ polymerization                     | Electrostatic deposition                                    |
| In-liquid drying                           | Centrifugal extrusion                                       |
| Thermal and ionic gelation in liquid media | Spinning disc at liquid/gas or solid gas interface          |
| Desolvation in liquid media                | Pressure extrusion or spraying into solvent extraction bath |

**Table 21.4** Commercial encapsulation processes and obtained capsule size (After [38]).

| Process                                 | Usual capsule size ( $\mu\text{m}$ ) |
|---|--------------------------------------|
| Spray drying                            | 5–5000                               |
| In-liquid drying or solvent evaporation | <1–1000                              |
| Polymer phase separation (coacervation) | 20–1000                              |
| Rotational suspension separation        | >50                                  |
| Fluidized bed (Wurster)                 | <100                                 |

Capsules produced by a chemical process are formed entirely in a liquid-filled stirred tank or tubular reactor. Mechanical processes use a gas phase at some stage of the encapsulation process.

In Table 21.4 the typical size of capsules produced is identified by a number of processes that have been commercialized.

### 21.3.2

#### Membrane Emulsification Devices

The various membrane emulsification procedure can be practised by using appropriate membranes and devices configuration.

The crossflow membrane emulsification can be obtained either with tubular or flat-sheet membranes, which are fixed in appropriate housing modules connected to circuits controlling fluid-dynamic conditions. A schematic drawing of a crossflow plant is reported in Figure 21.11. The figure also illustrates the tubular and flat-sheet membranes and modules. SPG (Japan) and Micropore (UK) were among the first companies producing plants for crossflow membrane emulsification. Figure 21.12 shows pictures of common marketed equipments.

Emulsification devices where the membrane is immersed in a stirred vessel containing the continuous phase, so as to obtain a batch emulsification device operating in deadend emulsification mode, have also been developed (Figure 21.13). Both flat-sheet and tubular membranes are used. In this membrane emulsification device, the continuous phase kept in motion creates the shear stress at the membrane surface that detaches the forming droplets. In a different operation mode, that is, when the continuous phase is not stirred, droplet formation in quiescent conditions is obtained.

Rotating membrane emulsification is another type of batch emulsification. In this case a tubular membrane immersed in a continuous phase vessel is rotating itself and its angular velocity creates the shear stress at the membrane surface (Figure 21.14).

Both crossflow and deadend systems can be used in premix and direct membrane emulsification. In the crossflow premix system the coarse emulsion is diluted by permeation into pure continuous phase/diluted emulsion recirculating at the low-pressure side of the membrane. In the deadend system the fine emulsion is withdrawn as a product after passing through the membrane, without any recirculation and/or dilution with the continuous phase. In this process, the fine emulsion can

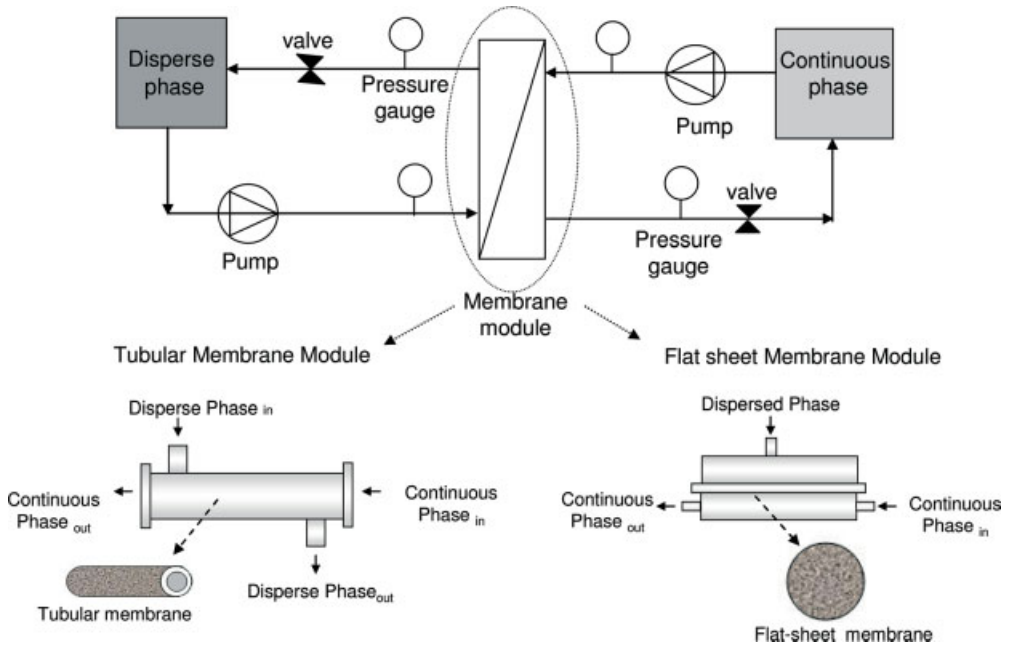
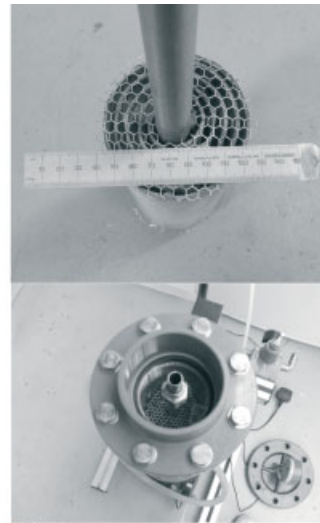


**Figure 21.11** Schematic drawing of a crossflow plant, using either tubular or flat-sheet membranes.



(a)



(b)

**Figure 21.12** Marketed equipments for membrane emulsification. (a) Plant for crossflow membrane emulsification produced by SPG Technologies Co. Ltd (<http://www.spg-techno.co.jp/>); (b) spiral-wound metallic membrane module produced by Micropore Technologies (<http://www.micropore.co.uk/>).

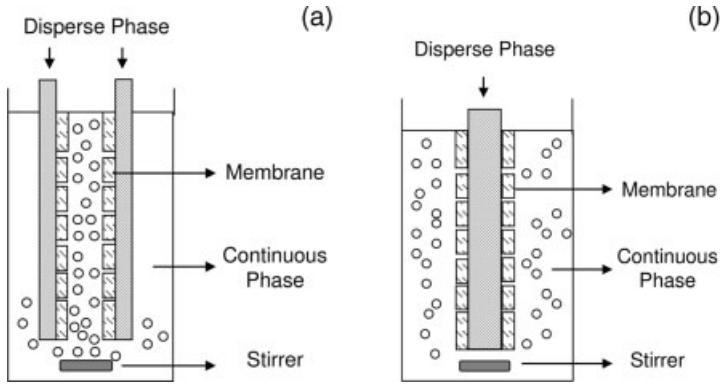


**Figure 21.13** Emulsification devices where the membrane is immersed in a stirred vessel containing the continuous phase. Transmembrane pressure applied from (a) external or shell side, and (b) internal or lumen side.

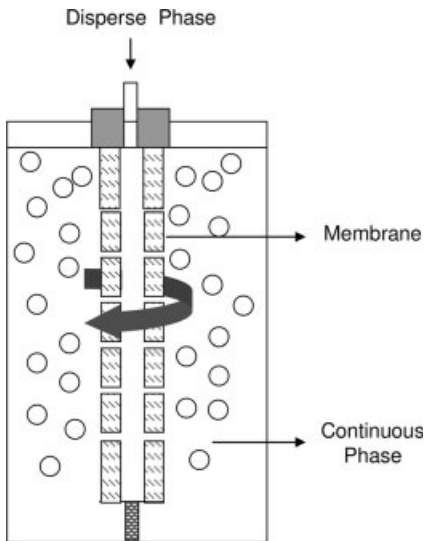


**Figure 21.14** Rotating emulsification device.

be repeatedly passed through the same membrane a number of times to achieve additional droplet-size reduction and enhance size uniformity (multipass premix membrane emulsification).

Each type of device has specific advantages and disadvantages. The batch emulsification is suitable for laboratory-scale investigations. The construction of the device is simple and handling during emulsification as well as for cleaning. Crossflow membrane emulsification is used when it is important that a proper adjustment of all process parameters and larger amounts of emulsion have to be produced.

A potential disadvantage of crossflow direct membrane emulsification is the relatively low maximum disperse-phase flux through the membrane ( $0.01\text{--}0.1\text{ m}^3/\text{m}^2\text{ h}$ ). Membrane, fluid properties, and transmembrane pressure determine the disperse-phase flux through the membrane. The opportune choice of membrane properties permits control of the flux during membrane emulsification process to be obtained. Due to the low productivity, that is, long production time, crossflow direct membrane emulsification is more suitable for the preparation of relatively diluted emulsions with disperse phase content up to 30%. Nevertheless, this process enables very narrow droplet-size distribution to be produced over a wide range of mean droplet size. Crossflow premix membrane emulsification holds several advantages over crossflow direct membrane emulsification. In fact, disperse-phase fluxes of the former emulsification process are typically above  $1\text{ m}^3/\text{m}^2\text{ h}$ , which is one to two orders of magnitude higher than the latter. In addition, the mean droplet sizes that can be achieved using the same membrane and phase compositions are smaller. Also, the experimental apparatus is generally simpler and the process is easier to control and operate since the driving pressure and emulsifier properties are not so critical for the successful operation as in crossflow direct membrane emulsification. One of the disadvantages of premix membrane emulsification is a higher droplet polydispersity.

#### 21.4 Theoretical Bases of Membrane Emulsification

From the theoretical point of view the key problem of the membrane emulsification is to explain and predict the dependence of the mean droplet diameter,  $D_d$  on the aforementioned membrane emulsification parameters. Important quantities such as droplet-formation time can thus be successively predicted by the mean droplet diameter and disperse-phase flux.

Droplet formation during direct membrane emulsification and in particular in crossflow emulsification has been described using models different in the scale and in the considered mathematical and physical phenomena, such as:

- (a) balance equations involving global forces,
- (b) surface free-energy minimization,
- (c) microscopic modeling using computational fluid dynamics (CFD) and lattice Boltzmann approaches.

The global balance models are less accurate than the other methods, however, they are easier to handle and more instructive. The latter feature is crucial to acquire the necessary understanding of the physical causes at the basis of the droplet formation and detachment. The balance methods are versatile and permit analysis of the influence of many membrane emulsification parameters with limited computational time, useful in process optimizations. Starting from these considerations, in this section more attention will be paid to the proposed torque and force balances.

The balances approaches have to necessarily incorporate approximations and fundamental hypotheses, which reduce the prediction capability of the latter. Every hypothesis comes from a postulated droplet-formation mechanism. The formation mechanism, however, depends significantly on the mentioned *operating, membrane and phase parameters*, thus, it is very difficult to find one mechanism valid for all possible parameters values. Consequently, more accurate computation procedures, such as the microscopic modeling or methods using the minimization of the droplet surface, are necessary for the detailed description of droplet formation and accurate predictions.

#### 21.4.1

##### Torque and Force Balances

This section breaks down as follows: first, the macroscopic forces acting on the droplet growing at the pore opening will be discussed, then the balance equations where these forces are involved will be dealt with. However, the accurate derivation of these forces is not reported here because it is beyond the aim of this contribution and therefore only the expressions of the forces used in balance equations will be presented.

The forces acting on a droplet attached to the pore opening can be conveniently subdivided into perpendicular and parallel direction with respect to the membrane surface. Considering the former case, the Young–Laplace  $F_{YL}$  [39] (named also static pressure force), the dynamic lift  $F_{DL}$  and buoyancy  $F_{BG}$  forces [26] are generally taken into account. They are defined as:

$$F_{YL} = \frac{\gamma}{D_d} \pi D_p^2 \quad (21.1)$$

$$F_{DL} = 0.761 \frac{\tau_{c,s}^{1.5} \rho_c^{0.5}}{\mu_c} D_d^3 \quad (21.2)$$

$$F_{BG} = \frac{1}{6} \pi g \Delta \rho D_d^3 \quad (21.3)$$

where  $D_p$  and  $D_d$  correspond to the average membrane pore and droplet diameter, respectively,  $\gamma$  is the liquid–liquid interfacial tension, while  $\tau_{c,s}$ ,  $\rho_c$  and  $\mu_c$  represent the shear stress, density and viscosity of the continuous phase, respectively. The quantity  $\Delta \rho$  in Equation 21.3 represents the difference between the continuous- and disperse-phase densities. However, various authors [13, 26] showed that for small pores (e.g., smaller than 2  $\mu\text{m}$ ), the  $F_{DL}$  and  $F_{BG}$  are negligible with respect the  $F_{YL}$ . The inertial force defined by the following equation 26:

$$F_I = \int_{A_p} \rho_d v_m^2 dA = \rho_d A_p v_m^2 \quad (21.4)$$

caused by the disperse-phase flow, with mean velocity  $v_m$ , would be another perpendicular force to consider. Here,  $A_p$  is the pore surface. Concerning the nature of this force, recently it has been emphasized [40] that it has a predominantly viscous

character rather than inertial. Starting from this observation, a more accurate expression of this hydrodynamic force has been determined. This force is explicitly dependent on the mean velocity of the disperse phase as well as of the pore diameter. The mean velocity of the disperse phase in turn depends on the effective pressure  $\Delta P_{\text{eff}}$ . Neglecting the pressure drop due to the membrane pore length,  $\Delta P_{\text{eff}}$  is equal to the difference between the transmembrane pressure and pressure drop necessary to overcome the capillary effect, that is the Laplace pressure [39]. To ensure monodisperse droplets and to avoid jets of the disperse-phase flux, the transmembrane pressure should never be markedly higher than the Laplace critical pressure. In these conditions, the  $\Delta P_{\text{eff}}$  produces a small mean velocity and a negligible inertial force or hydrodynamic force with respect to  $F_{\text{YL}}$  and the drag force. The general expression used to consider the drag force  $F_{\text{DR}}$  [13, 26, 39] due to the continuous-phase crossflow and parallel to membrane surface is the following:

$$F_{\text{DR}} = \frac{3}{2} k_x \pi \tau_{\text{c,s}} D_d^2 \quad (21.5)$$

where the parameter  $k_x$  is equal to 1.7 and takes into account the wall correction factor for a single sphere touching an impermeable wall [41]. In Equation 21.5, the approximation  $v_{\mu_c} \approx (1/2) \tau_{\text{c,s}} D_d$  is adopted, where  $v$  is the undisturbed crossflow velocity. The shear stress, evaluated at the droplet center, is assumed equal to that at the membrane surface, which is the wall shear stress. Referring to the expression 21.5, two important considerations are necessary. The first concerns the disperse-to-continuous viscosity ratio. In fact, in Equation 21.5 is only considered the viscosity of the continuous phase because this expression is Stocks's law corrected to account for the interaction with the membrane surface. Nevertheless, the disperse-to-continuous viscosity ratio can significantly affect the values of the effective drag force [42]. This consideration is connected with the droplet deformability; the solid particle approximation (Stocks's law) can be a restricted assumption in direct membrane emulsification modeling. The second observation concerning the  $F_{\text{DR}}$  is connected with the value of the wall correction factor parameter  $k_x$ . The reported value was obtained considering a solid droplet leaned on a surface, this assumption should be improved in the case of a droplet growing from a pore. Although different  $F_{\text{DR}}$  are presented in the literature [43], the wall shear stress at the membrane surface always appears explicitly in these expressions. This quantity depends on the membrane geometry and module. For simple modules (e.g., tubular or flat) consolidated expressions of the wall shear stress can be found [39]. For more complex equipments holding the membrane (e.g., rotating or vibrating systems), the evaluation of the shear stress requires more complicated analysis and calculations [43]. A particular consideration is necessary for the vibrating systems. Recently, it has been emphasized [44] that vibrations of the membrane introduces additional inertial and drag forces (secondary drag force) in a direction parallel to the membrane surface. These two forces depend on the excitation amplitude and the excitation frequency.

All presented forces are detaching forces. An increase in these forces will decrease the diameter of the droplets. On the contrary, the interfacial force caused by a uniform interfacial tension along the pore border is a holding force; increasing this force will

increase the droplet size. The more simple and common expression of this force is [13, 39, 45] defined as:

$$F_\gamma = \pi D_p \gamma \sin \theta \tag{21.6}$$

where  $\theta$  represents the contact angle. The capillary force 21.6 is obtained by the integration along the pore perimeter of the  $dF_\gamma$ , force acting on  $dL$  of the pore border. The force  $dF_\gamma$  has magnitude  $\gamma dL$  and is directed towards the pore. The contact angle  $\theta$  is assumed constant in the integration. This constraint could be a severe approximation. In fact, the droplet, during its formation, could counterbalance the actions due to the continuous fluid crossflow and  $F_{YL}$ ,  $F_{DL}$ ,  $F_{BG}$ , and  $F_I$  forces by changing its contact angle along the pore border, that is the droplet twists on the surface. The droplet inclination yields an interfacial force sufficient to keep the droplet on the membrane. Thus, the global  $F_\gamma$  should be rewritten in order to take into account the change of contact angle on the contact line [46]. This interfacial force can be expressed as sum of the two components  $F_{\gamma i}$  and  $F_{\gamma k}$ . Considering the contact line  $\Gamma$  of generic size and shape, the interfacial force can be defined according the following two components:

$$F_{\gamma i} = \int_\Gamma \gamma (\mathbf{M} \cdot \mathbf{m}) \mathbf{m} \cdot \mathbf{i} d\Gamma \quad \text{parallel to the membrane surface}$$

$$F_{\gamma k} = \int_\Gamma \gamma (\mathbf{M} \cdot \mathbf{k}) \mathbf{k} \cdot \mathbf{k} d\Gamma \quad \text{perpendicular to the membrane surface}$$

(21.7)

where  $\mathbf{M}$  and  $\mathbf{m}$  are the unit vectors, whose directions are indicated in Figure 21.15.

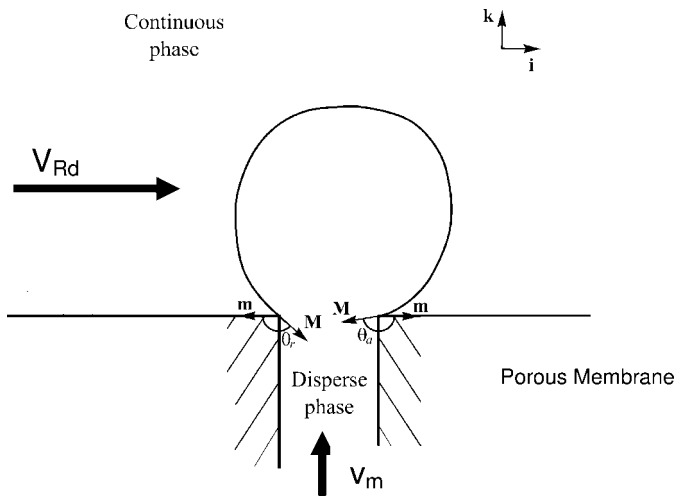


**Figure 21.15** Droplet formation at the pore opening. Side view with vectors indicating the unit vectors,  $\mathbf{M}$  and  $\mathbf{m}$  at the pore perimeter and the advancing ( $\theta_a$ ) and receding ( $\theta_r$ ) contact angles.  $V_{Rd}$  represents the crossflow velocity of continuous phase at height equal to droplet radius, and  $v_m$  is the mean disperse-phase velocity.

Concerning the shape of  $\Gamma$ , it should be noted that the droplet contact line does not necessarily coincide with the pore border. In fact, depending on the affinity between the membrane and the disperse phase, the droplet can spread around the pore. Using the definition for the contact angle  $\cos \theta = \mathbf{M} \cdot \mathbf{m}$ , Equation 21.7 yields the components of the interfacial tension as a function of the contact angle along the contact line  $\Gamma$ . The integration in Equation 21.7 can be conveniently carried out by dividing the contact line into four sections: the advancing ( $\Gamma_a$ ) and receding ( $\Gamma_r$ ) portions, along which the contact angles assume the constant values  $\theta_a$  and  $\theta_r$ , respectively, and the two lines corresponding to the transition zones (TZ) in which the contact angles are not constant. Thus, Equation 21.7 can be expanded in a more easy to handle form as:

$$\begin{aligned} F_{\gamma i} &= \gamma \cos \theta_a \int_{\Gamma_a} \mathbf{m} \cdot \mathbf{i} d\Gamma + \gamma \cos \theta_r \int_{\Gamma_r} \mathbf{m} \cdot \mathbf{i} d\Gamma + 2\gamma \int_{TZ} \cos \theta(\Gamma) \mathbf{m} \cdot \mathbf{i} d\Gamma \\ F_{\gamma k} &= \gamma \sin \theta_a \Gamma_a + \gamma \sin \theta_r \Gamma_r + 2\gamma \int_{TZ} \sin \theta(\Gamma) d\Gamma \end{aligned} \quad (21.8)$$

It is worth noting that if  $\theta_a$  and  $\theta_r$  are equal to the equilibrium contact angle  $\theta$ , then the first component becomes zero, whereas the second component reduces to the above Equation 21.6. For more information on the difference between  $\theta_a$ ,  $\theta_r$  and equilibrium contact angle given by the Young equation the reader may refer to the original works [46, 47].

The presented forces are used in different balance equations according to mechanics assumptions. From the mechanics point of view two possible states for an immiscible droplet injected into a liquid continuous phase can be considered: (a) the droplet may maintain a spherical symmetry until it begins its detachment (rigid spherical cap configuration) and here the most appropriate mechanical model would be a torque balance, and (b) a deformed droplet at its base, where a force balance at the pore perimeter would be the most suitable model. Both the torque and force balances can be used to derive equations that will define the diameter of the droplet before its detachment. To be able to calculate the instant when the droplet has grown sufficiently to detach from the pore, Peng and Williams [13] at first suggested a torque balance around a pore edge:

$$F_{DR} h = (F_{\gamma} - F_{YL} - F_{BG}) \frac{D_p}{2} \quad (21.9)$$

in which  $h$  is the droplet height from the membrane surface. If the droplet shape is significantly deformed towards the membrane then  $h$  can be approximated with the pore radius and Equation 21.8 reduces to:

$$F_{DR} = (F_{\gamma} - F_{YL} - F_{BG}) \quad (21.10)$$

In Equations 21.9 and 21.10, the interfacial force 21.6 is used by employing a contact angle equal to  $\pi/2$ . Generally in Equation 21.9 the droplet height is substituted by the droplet radius,  $D_d/2$ . These equations permit calculation of which diameter torques in clockwise and anticlockwise directions are balanced, beyond this value the droplet detaches. However, for a short period the droplet still maintains its

connection with the pore through a neck. When this connection is completely broken the droplet detachment is complete 48. Kelder *et al.* and van Rijn [44, 49] used a force balance equation to predict the *final* droplet diameter, that is the droplet size at the end of its detachment. In their model the droplet is attached at the pore border by a curved neck (similar to a strap). The droplet is not leaned on the pore opening but on the membrane surface. Combining Equations 21.6 and 21.5 yields the following force-balance equation:

$$F_{DR} = F_{\gamma} \quad (21.11)$$

Although the last two balances are similar, it is worth noting that from the mechanics point of view they are different. In fact, the first derives from an approximation on the droplet height, whereas the second derives from a different droplet configuration with respect to the membrane surface. The first balances (Equations 21.9 and 21.10) estimate the droplet volume at the beginning of the detachment, whereas the second balance (Equation 21.11) estimates it at the end of the detachment (*final droplet dimension*). The  $F_{DR}$  used by Kelder *et al.* is acting on the center of the droplet, thus it is not expressed as a function of the wall shear stress. However, in both force balances, the holding force 21.6 is used as the interfacial force. De Luca and Drioli [46] at first proposed a balance force model along the droplet contact line  $\Gamma$  using the interfacial force 21.8 instead of Equation 21.6. Components of the interfacial force 21.8 have to counterbalance both the drag force and the forces in the direction perpendicular to membrane surface (all the detaching forces). The droplet deformability is taken into account through the evaluation of the advancing and receding contact angles along the droplet–pore contact line. The detachment is supposed to occur when the interfacial force at the droplet base is unable to counterbalance, through the droplet inclination, the actions of the detaching forces. The resultant set of force balance equations is:

$$\begin{cases} F_{\gamma i}(\theta_a, \theta_r) + F_{DR} = 0 & \text{parallel to the membrane surface} \\ F_{\gamma k}(\theta_a, \theta_r) + F_{YL} + F_{DL} + F_{BG} = 0 & \text{perpendicular to the membrane surface} \end{cases} \quad (21.12)$$

where the dependence of the interfacial tension force on the contact angles is reported for clarity. This set of equations can be solved at every droplet diameter to find the contact angles providing the equilibrium of forces. The solution of Equation 21.12 is the set of  $\theta_a$  and  $\theta_r$  values for any value of the droplet diameter chosen as parameter. The solution paths are in all cases closed lines lying within a minimum and maximum  $D_d$  value corresponding to the initial pore diameter ( $D_0 > D_p$ ) and critical value denoted by  $D_c$  (*critical droplet diameter*), respectively. Since no solution exists for a droplet diameter larger than  $D_c$ , then it is concluded that this value has the meaning of droplet diameter corresponding to which the detachment of the droplet starts. In those cases where solution branches are found to be physically unacceptable,  $D_c$  is taken to be the smallest diameter corresponding to one of the two contact angles reaching the value of  $\pi$ . It is worth noting that if for particular  $\theta_a$  and  $\theta_r$  values the first equation in the balances 21.12 is not satisfied but the second equation could be satisfied, the droplet should glide along the surface without

detaching from the membrane. Recently, Christov *et al.* [17] have proposed a balance-force equation similar to the balance 21.11 but for the droplet detachment in quiescent conditions. In this model the interfacial force 21.6, corrected with the Harkins-Brown factor  $f_{\text{d}}$ , is counterbalanced by the hydrodynamic force that substitutes the drag force  $F_{\text{DR}}$ . Using an appropriate expression for the mean velocity of the disperse phase defining the hydrodynamic force, the authors proposed a balance equation between these two forces. It is worth noting that in quiescent conditions and for a spherical disperse/water interface (i.e., a spherical sector), the Young-Laplace force 21.1 is always balanced for a contact angle equal to  $\arcsin(D_{\text{p}}/D_{\text{d}})$ . Therefore, in this condition the hydrodynamic force could be the driving force for the droplet detachment.

The last consideration of this section concerns the coupling effects occurring in membrane emulsification. The adsorption of the emulsifier on the droplet interface changes the values of the interfacial tension and consequently the interfacial force [26, 50, 51]. In addition, the equilibrium contact angle  $\theta_{\text{c}}$  changes as the emulsifier is adsorbed. As shown by [26, 50, 51] the effects of emulsifier adsorption depend on the ratio between droplet-formation time and emulsifier adsorption rate. If the droplet-formation time is large enough to permit a complete adsorption of emulsifier then the equilibrium interfacial tension can be used in the above force expressions. On the contrary, if the droplet-formation process is not large enough then the dynamic interfacial tension function has to be considered as a substitute for the scalar equilibrium interfacial tension. In this case the coupling between the droplet diameter and dynamic interfacial tension has been introduced in the correlated balance equations [50].

#### 21.4.2

##### Surface-Energy Minimization

Rayner *et al.* [52] analyzed the formation mechanism of a droplet from a single pore into a quiescent continuous phase condition evaluating the dimensionless Reynolds, Bond, Weber, and the capillary numbers. The magnitude of these dimensionless numbers was calculated for the following membrane emulsification setup: 1  $\mu\text{m}$  pore diameter, 5 mN/m interfacial tension,  $8 \times 10^2 \text{ kg/m}^3$  oil density,  $5 \times 10^{-3} \text{ Pa s}$  viscosity and  $1 \times 10^{-3} \text{ m/s}$  disperse-phase velocity and zero continuous-phase velocity. The above dimensionless numbers indicate that the interfacial force 21.6 absolutely dominates the emulsification process; the hydrodynamic force due to the disperse-phase flow is negligible and the drag force absent. In other terms, the holding interfacial force always balances the other involved forces until the complete detachment of the droplet due to a spontaneous deformation. Thus, the balance (Equations 21.9–21.12) is not predictive in this case because the deformation of the droplet is not included.

Starting from this consideration, Rayner *et al.* [52] analyzed the spontaneous-transformation-based (STB) droplet-formation mechanism from the point of view of the surface Gibbs free energy with the help of the Surface Evolver code. Rayner *et al.* estimated the difference of surface free energy of the droplet before ( $E_1$ ) and after ( $E_2$ )

its detachment,  $E_2 - E_1$ . When  $E_1$  is larger than  $E_2$  then the spontaneous droplet formation begins. Surface Evolver code was used to evaluate  $E_1$  energy. In particular, for an assigned disperse–continuous–surfactant interfacial tension, Surface Evolver, for each droplet volume attached at the pore perimeter, yields the droplet surface with the minimum energy among the possible surfaces related with the given volume. This minimization must respect important constraints, that is the geometry of the pore border and the equilibrium contact angle that is set as a contact energy around the pore. Once the minimum  $E_1$  energy is found, the  $E_2$  energy have to be evaluated. The  $E_2$  value is the free energy of the detached droplet having the same volume of the attached droplet plus the energy of the pore opening. The maximum stable droplet volume (MSV) is the volume of the attached droplet just before the STB droplet formation takes place, that is when  $E_1 > E_2$ . Surface Evolver also gives the possibility to find the maximum stable droplet volume thought the Hessian eigenvalues analysis. The occurrence of negative eigenvalues corresponds to the point at which the  $E_2 - E_1$  difference becomes negative. The MSV yields an estimation of the largest droplet that should be formed. It is well known that there is a certain volume of disperse phase remaining attached at the pore. Rayner *et al.* estimated this remaining volumes using the ‘pressure pinch constraint’ principle. This principle is based on the division of the droplet MSV into two parts having relative sizes that show an equal Laplace pressure across the surface of both volumes. Using this principle the authors yielded an estimation of the droplet diameters in quiescent conditions and for very low disperse-phase flow. The Rayner *et al.* approach estimates the maximum dimension achievable for the droplet. The Surface-Evolver-based simulations also showed that for pores with aspect ratio (maximum to minimum length) greater than three the necking formation should occur inside the pore. On the contrary, when the aspect ratio is smaller than three the droplet necking took place outside the membrane pore. The same authors [53] used this approach to analyze the effect of the dynamic surfactant coverage on the final droplet size coupled to the expansion rate of the continuous/disperse interface. They found that the dynamic surfactant coverage has a significant influence on the final droplet size during the analyzed membrane emulsification process.

### 21.4.3

#### **Microfluid Dynamics Approaches: The Shape of the Droplets**

In the microfluid dynamics approaches the continuity and Navier–Stokes equation coupled with methodologies for tracking the disperse/continuous interface are used to describe the droplet formation in quiescent and crossflow continuous conditions. Ohta *et al.* [54] used a computational fluid dynamics (CFD) approach to analyze the single-droplet-formation process at an orifice under pressure pulse conditions (pulsed sieve-plate column). Abrahamse *et al.* [55] simulated the process of the droplet break-up in crossflow membrane emulsification using an equal computational fluid dynamics procedure. They calculated the minimum distance between two membrane pores as a function of crossflow velocity and pore size. This minimum distance is important to optimize the space between two pores on the membrane

surface (i.e., the membrane porosity) in order to avoid droplet coalescence on the surface. They characterized the mechanism of the droplet formation (droplet shape, pressure drop through the pore, etc.) occurring for the assigned conditions. Quite recently, Kobayashi *et al.* [56] carried out a numerical investigation on the formation of an oil droplet in water from straight-through microchannels (MC) with an elliptic cross-section and in quiescent conditions. In particular, these CFD simulations demonstrated that the neck formation considerably depends on the aspect ratio of the elliptic MC. Continuous outflow of the oil phase from the channel opening was observed for elliptic MCs below a threshold aspect ratio between 3 and 3.5. On the contrary, a droplet with neck inside the membrane pore was found for a droplet formed in the elliptic MCs exceeding the above threshold aspect ratio. This result is in agreement with the conclusion found by Rayner *et al.* [52] reported above. Cristini and Tan recently reviewed numerical simulations of droplet dynamics in complex flows [57].

The computational fluid dynamics investigations listed here are all based on the so-called volume-of-fluid method (VOF) used to follow the dynamics of the disperse/continuous phase interface. The VOF method is a technique that represents the interface between two fluids defining an  $F$  function. This function is chosen with a value of unity at any cell occupied by disperse phase and zero elsewhere. A unit value of  $F$  corresponds to a cell full of disperse phase, whereas a zero value indicates that the cell contains only continuous phase. Cells with  $F$  values between zero and one contain the liquid/liquid interface. In addition to the above continuity and Navier–Stokes equation solved by the finite-volume method, an equation governing the time dependence of the  $F$  function therefore has to be solved. A constant value of the interfacial tension is implemented in the summarized algorithm, however, the diffusion of emulsifier from continuous phase toward the droplet interface and its adsorption remains still an important issue and challenge in the computational fluid-dynamic framework.

The CFD procedures briefly presented are a valid tool for an accurate *in-silico* analysis of the droplet-formation mechanisms occurring under various membrane emulsification parameters. This knowledge can be used in the formulation and validation of the basic assumptions characterizing the aforementioned balance models. Validated computation fluid dynamic models are useful to design optimal membranes and related equipments. In other words, the CFD procedure can be used for *in-silico* experiments avoiding expensive experimental trial and error tests. Nevertheless, it is worth noting that the CFD simulations for membrane emulsification processes are time-consuming tasks. This aspect can be restrictive if many *in-silico* experiments have to be carried out. Although the CFD procedures give useful information on the droplet break up, not all phenomena are modeled on a solid physical basis, which can result in ambiguous conclusions as in the case for the modeling the contact line dynamics. Other CFD approaches that do not use the VOF procedure (e.g., level-set procedure) should be taken into account. However, this approach in the membrane emulsification is still at an early stage of development.

Lattice Boltzmann (LB) is a relatively new simulation technique and it represents an alternative numerical approach in the hydrodynamics of complex fluids. The LB method can be interpreted as an unusual finite-difference solution of the continuity

and Navier–Stokes equation and it is suitable for modeling of multiphase systems. The LB is based on hypothetical fluid particles (packages of fluid) moving and colliding on a lattice according to the kinetic gas theory. One of the most important reasons why the LB algorithm works well for multiphase problems is that the interfaces appear and move automatically during the simulation. By contrast to the mentioned CDF method, it is not necessary to track the interface explicitly. In addition, the implementation of complex wetting conditions (e.g., patterned surfaces) and the dynamics of contact line turns out to be more simple and accurate with respect to the traditional CFD approaches. Moreover, the diffusion and dynamic adsorption of emulsifiers during the droplet formation is another aspect that can be correctly treated in a LB framework. In general, the LB simulations for membrane emulsification processes are less intensive (time consuming) with respect to the analogous CFD ones. Although the LB methodology has found applications in different areas of fluid dynamics, including simulations of flows in porous media and droplet formation in liquid–gas systems [58], at the moment only the work of van der Graaf *et al.* [18] is addressed to the droplet formation from a T-shaped microchannel in a liquid–liquid system. It is worth noting that the T-shaped microchannel geometry was approximated as a model of a membrane pore.

Although the premix membrane emulsification can yield larger fluxes with respect to direct membrane emulsification neither methods using surface-energy minimization nor microfluid dynamics approaches have been until now reported on the theoretical treatment of the premix membrane emulsification.

## 21.5 Membrane Emulsification Applications

### 21.5.1 Applications in the Food Industry

Emulsions play an important role in the formulation of foods, that is, o/w emulsions are used for preparation of dressings, artificial milks, cream liqueurs, and w/o emulsions are used in the production of margarines and low-fat spreads.

Food products must have appropriate texture properties. For example, it is important that mayonnaise products have thick and creamy textures, but not too high a viscosity. The rheological properties depend on their composition, such as the concentration of oil droplets or the concentration of thickening agents.

The development of membrane emulsification technologies permits production of small and uniform droplets and capsules, using mild conditions of temperature, shear stress and pressure. Furthermore, they are able to produce stable droplets with reduced stabilizers content, which will contribute to the manufacturing of improved food products with low-fat content.

In this context, the Morinaga Milk Industry (Japan) developed and commercialized a very low fat spread using membrane emulsification technology [59, 60]. The advantages in the production of low-fat spreads made the process one of the first

large-scale applications of membrane emulsification. A w/o emulsion using a MPG hydrophilic membrane, previously treated with the oil phase, has been prepared by crossflow membrane emulsification. The resulting product was stable and free from aqueous phase separation, tasted smooth and melted extremely easily in the mouth.

For practical applications in the food industry, where large-volume production is conducted, it is especially important to obtain high disperse-phase flux. Abrahamse *et al.* [8] reported on the industrial-scale production of culinary cream. In this study they evaluated the required membrane area for different types of membranes: an SPG membrane, an  $\alpha$ -Al<sub>2</sub>O<sub>3</sub> membrane and a microsieve filter. The requirements for culinary cream production were: a droplet size between 1 and 3  $\mu\text{m}$  and a production volume of 20 m<sup>3</sup>/h containing 30% disperse phase. They concluded that to produce large quantities of monodisperse emulsions the most suitable was a microsieve with an area requirement of around 1 m<sup>2</sup>.

Katoh *et al.* [3] prepared w/o emulsions composed of salt solution, polyglycerin polyricinolate (PGPR) at 2%wt and corn oil. It has been proven that the disperse-phase flux was increased 100-fold using a hydrophilic membrane pretreated by immersion in the oil phase. This made the membrane emulsification system practical for large-scale production of a w/o emulsion in food application.

Double emulsions are also very useful for food application. Sensitive food materials and flavors can be encapsulated in w/o/w emulsions. Sensory tests have indicated that there is a significant taste difference between w/o/w emulsions and o/w emulsions containing the same ingredients, and that there is a delayed release of flavor in double emulsions [61]. W/o/w or o/w/o multiple emulsions having a concentrated aqueous-soluble flavor or a concentrated oil-soluble flavor encapsulated in the internal phase can be prepared. Food products obtained with these particulates exhibit enhanced flavor perception and extended shelf-life [62].

### 21.5.2

#### Applications in the Pharmaceutical Industry

Among the applications of membrane emulsification, drug-delivery system (DDS) is one of the most attractive fields. W/o/w emulsions have been prepared to transport and deliver anticancer drug [4, 63–65]. The emulsion was directly administered into the liver using a catheter into the hepatic artery. In this way, it was possible to suppress the strong side effects of the anticancer drug and also concentrate the dosage selectively to focus on the cancer. The clinical study showed that the texture of the cancer rapidly contracted and its volume decreased to a quarter of its initial size.

Composite emulsion as carrier of hydrophilic medicine for chemotherapy was prepared by adding albumin to the internal water phase and lecithin or cholesterol to the oil phase, thus obtaining a water-in-oil emulsion. This emulsion was then pressed through Millipore membrane into an external water phase to form a w/o/w multiple emulsion. Its advantages are high size uniformity and high storage stability [66].

Nakajima *et al.* referred to membrane emulsification as a method to make functional ethanol-in-oil-in-water (e/o/w) emulsions. These e/o/w emulsions are suitable to encapsulate functional components that have a low water and oil solubility

while being soluble in ethanol. An example is taxol, which is an anticancer terpenoid [67].

Vladisavljevic *et al.* reported on the production of multiple w/o/w emulsions for drug-delivery systems by extruding a coarse w/o/w emulsion five times through a SPG membrane [68].

Several studies also reported on the preparation of biodegradable polymer microcapsules to be used as drug-delivery systems due to their biodegradable nature and proven biocompatibility. The biopolymers employed are mainly poly(lactide) (PLA) [69], poly(lactic-co-glycolic acid) (PLGA) [70–74], chitosan [75, 76], and calcium alginate [77]. Such polymers have been applied for encapsulating proteins and peptides used as prophylactic and therapeutic agents in biomedical fields. So far, the delivery route is injection, which not only causes distress and inconvenience to patients, but also induces unstable curative effective and side effects. This is due to the fact that the drugs have to be given frequently, resulting in rapid increase and decrease of drug concentration in blood [75]. Therefore, a sustained delivery system for proteins and peptides is necessary not only for injection administration but also for developing an oral-administration system. The use of microspheres as a controlled release system is one of the prospective methods. In fact, it may prevent encapsulated drugs from degradation by proteolytic enzymes, prolong its half-life and improve its bioavailability *in vivo* by controlling the release rate of the drug from the microspheres.

The preparation of monodisperse hydrogel microspheres, such as poly-acrylamide-co-acrylic acid, poly(N-isopropylacrylamide-co-acrylic acid), has been performed for drug devices thanks to their biocompatibility [77, 79]. The average diameters of the microspheres were dependent on the pore sizes (from 0.33 to 1.70  $\mu\text{m}$ ) of SPG membranes used in the preparation procedure.

Solid lipid nanoparticles (SLN) have also been introduced as an alternative to solid particles, emulsions and liposomes in cosmetic and pharmaceutical preparations. Charcosset *et al.* reported the use of membrane emulsification for the production of SLN [80]. The lipid phase was pressed through the membrane pores into the aqueous continuous phase, at a temperature above the melting point of the lipid. The SLN are then formed by the following cooling of the preparation to room temperature. The lipids remain solid also at body temperature. The influence of process parameters on the size and the lipid-phase flux was investigated. The membranes used were supplied by Kerasep ceramic membranes with an active  $\text{ZrO}_2$  layer on an  $\text{Al}_2\text{O}_3$ - $\text{TiO}_2$  support. Three different microfiltration membranes were investigated: 0.1, 0.2, and 0.45  $\mu\text{m}$  mean membrane pore size. It was shown that SLN nanoparticles could be prepared with a liquid-phase flux between 0.15 and 0.35  $\text{m}^3/\text{h m}^2$  and mean SLN size between 70 and 215 nm.

### 21.5.3

#### Applications in the Electronics Industry

The membrane emulsification technique is also employed for the preparation of microspheres starting from monomers such as methacrylates (methylmethacrylate, cyclohexyl acrylate, etc.), polyimide prepolymer, styrene monomer [81], and so on.

The occlusion of functional materials such as the polyimide prepolymer (PIP) in uniform polymer particles, can find promising applications in sophisticated electronic devices such as adhesive spacers of liquid-crystal panel boards (after a minor screening process), adhesives or insulators for microtip circuits, and so forth. Omi *et al.* [82] showed that about 30% occlusion of polyimide prepolymer (diphenylmethane-4,4'-bis-allyl-nagiimide, BAN-I-M) was accomplished in the preparation of polymer particles composed of styrene, various acrylates and a crosslinking agent (ethyleneglycol dimethacrylate, EGDMA) via the emulsification technique with SPG membrane. Particles with a diameter of 6–12 micrometers were prepared. The presence of acrylates and EGDMA was essential to obtain stable lattices of styrene-based copolymers that occlude BAN-I-M. However, the presence of acrylates with longer side chains, BA and 2EHA, promoted the inclusion of BAN-I-M. In particular, the latter yielded a stable latex occluding 100% of the initial BANI-M without the crosslinking matrix and using octyl alcohol as a stabilizing agent. The lattices without a crosslinking network resulted in an excellent adhesive ability.

Guang Hui Ma *et al.* [83] prepared microcapsules with narrow size distribution, in which hexadecane (HD) was used as the oily core and poly(styrene-co-dimethylamino-ethyl methacrylate) [P(st-DMAEMA)] as the wall. The emulsion was first prepared using SPG membranes and a subsequent suspension polymerization process was performed to complete the microcapsule formation. Experimental and simulated results confirmed that high monomer conversion, high HD fraction, and addition of DMAEMA hydrophilic monomer were three main factors for the complete encapsulation of HD. The droplets were polymerized at 70 °C and the obtained microcapsules have a diameter ranging from 6 to 10  $\mu\text{m}$ , six times larger than the membrane pore size of 1.4  $\mu\text{m}$ .

Furthermore, such monomers can be readily emulsified by dissolving in volatile solvents such as methylene chloride and chloroform. Uniform polylactide particles, and composite polystyrene (PST) and polymethyl methacrylate (PMMA) particles were produced by solvent evaporation [84–86].

#### 21.5.4

#### Other Applications

Membrane emulsification has also been applied for the preparation of oil-in-water emulsions to be used in cosmetics and/or dermatology, in particular for the treatment, protection, care, cleaning and make-up of the skin, mucous membranes and hair. The emulsion was composed by oil-phase globules having an average size less than 20  $\mu\text{m}$ ; it was prepared by direct membrane emulsification through a porous hydrophilic glass membrane having an average pore size ranging from 0.1 to 5  $\mu\text{m}$  and preferably from 0.3 to 3  $\mu\text{m}$  [87].

The technology also represents a suitable strategy for the preparation of multi-phase reaction systems that use phase transfer (bio)catalysts. Giorno *et al.* [88] reported on the use of membrane emulsification to distribute lipase from *Candida rugosa* at the interface of stable oil-in-water emulsions. The enzyme itself was used as a surfactant. Shirasu Porous Glassy (SPG) membranes having a nominal pore

diameter of 0.1  $\mu\text{m}$  were used to prepare emulsions. Emulsions with more than 90% of organic droplets of 1.6 ( $\pm 0.40$ )  $\mu\text{m}$  were obtained. The methodology allowed preservation of the catalytic performance of the biocatalyst as well as optimal enzyme distribution at the interface of stable, uniform and small oil droplets to be achieved.

Applications in the chemical field, include extrusion of an oil phase containing a photographic hydrophobic material through a microporous membrane into water [89] and emulsification of low-viscosity paraffin wax in water [90].

The polyurethane (PU) can be considered an environment-friendly material because the urethane bond resembles the amide bond, which implies possible biodegradability. It can be used in various elastomer formulations, paints, adhesives for polymers and glass, and artificial leather as well as in biomedical and cosmetic fields. Polyurethane spheres were prepared from 20/40% of PU prepolymer solution in xylene [91]. PU droplets were formed in water with the SPG membrane of different pore size (1.5–9.5  $\mu\text{m}$ ) and then polymerized to form the final microspheres. Finally, spherical and solid PU particles of 5  $\mu\text{m}$  were obtained after the removal of the solvent. In another study, Ma *et al.* reported the formation of uniform polyurethane-vinylpolymer (PUU-VP) hybrid microspheres of about 20  $\mu\text{m}$ , prepared using SPG membranes and a subsequent radical suspension polymerization process [92]. The prepolymers were solubilized in xylene and pressed through the SPG membrane into the continuous phase containing a stabilizer to form uniform droplets. The droplets were left for chain extension at room temperature for some hours with di- and triamines by suspension polymerization at 70 °C for 24 h. Solid and spherical PU-VP hybrid particles with a smooth surface and a higher destructive strength were obtained.

Ha *et al.* [93, 94] prepared monodisperse polymer microspheres from 1 to 40  $\mu\text{m}$  in diameter for medical diagnostic tests, as chromatography column packing and as calibration standards. The work deals with the synthesis of large and uniform poly (butadiene-styrene) latex. The ceramic SPG membrane, with a pore diameter of 1.6  $\mu\text{m}$ , was employed. The uniform particle sizes were in the diameter range of 4–6  $\mu\text{m}$ .

Westover *et al.* [95] prepared lightly crosslinked nitrated poly(4-hydroxystyrene) microspheres for pH sensors. The microspheres were produced using SPG membranes followed by suspension polymerization and they showed diameters between 1 and 2 micrometers.

Figoli *et al.* [96, 97] reported the preparation of polymeric capsules combining the phase-inversion technique with the membrane process. Polyetheretherketone (PEEKWC) capsules of different size (300–800 micrometer) and morphology (asymmetric with a porous or dense layer) have been prepared. The SEM pictures of the prepared PEEKWC capsules are shown in Figure 21.16. The capsules can find application both in chemical and in food packaging fields [98].

Another field where emulsions are likely to become imperative is the production of fuel [99]. Simple and multiple emulsions represent alternative fuels for diesel engines to both increase combustion efficiency and reduce particulate emission. Considering the enormous volume of diesel that is being consumed today, a replacement of just a fraction of regular diesel by diesel emulsion could be of considerable interest to the surface chemistry community. Until now, diesel emulsions were prepared by

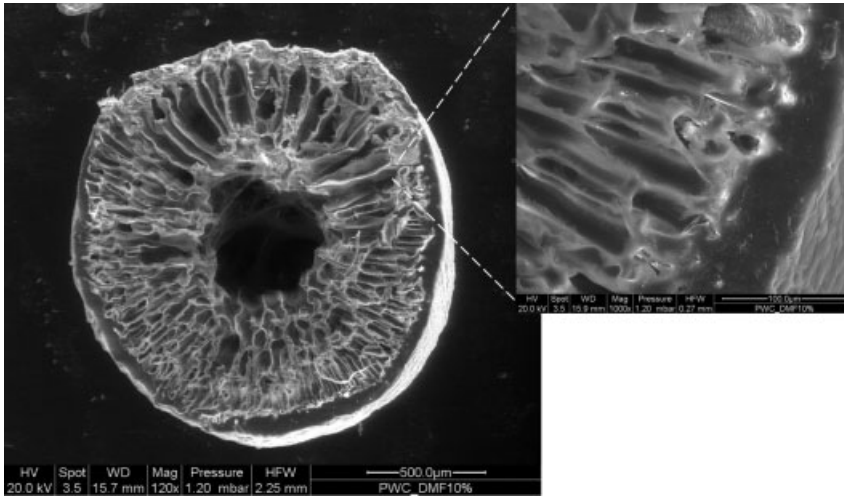


**Figure 21.16** SEM pictures of the crosssection of the PEEKWC capsules prepared by the phase-inversion technique using a film with a pore size of  $550\ \mu\text{m}$  [97].

conventional emulsification methods but it is expected that the membrane emulsification technique will also become attractive for this application.

## 21.6 Conclusions

Membrane emulsification, a technology that first appeared in the early 1990s, is gaining increasing attention with many applications being explored in various fields. Nowadays, it can be considered at a developing/exploiting stage with a significant involvement of industrial and academic research effort. Many studies have been carried out, especially from the experimental point of view whereas from the theoretical point of view the knowledge is not accordingly advanced.

In this chapter, a description of membrane emulsification basic concepts, empirical correlations, theoretical studies, as well as most common applications have been discussed.

Many patents have been applied for, especially in Japan, which currently holds more than 60% of worldwide applications, in Europe and USA.

Main drivers for membrane emulsification development include high product quality – especially when labile molecules are involved, precise definition of droplet-size distribution, low energy input, equipment modularity and easy scale-up, and low equipment footprint.

Challenges in this field include the need for higher productivity, membranes and modules specifically designed for the emulsification process, modules construction standardization, and design of innovative intensified processes.

## References

- 1 Nakashima, T., Shimizu, M. and Kukizaki, M. (1991) *Membrane Emulsification Operation Manual*, 1st edn, Industrial Research Institute of Miyazaki Prefecture, Japan.
- 2 Nakashima, T. and Shimizu, M. (1991) *Key Engineering Materials*, **61/62**, 513–516.
- 3 Katoh, R., Asano, Y., Furuya, A., Sotoyama, K. and Tomita, M. (1996) *Journal of Membrane Science*, **113** (1), 131–135.
- 4 Nakashima, T., Shimizu, M. and Kukizaki, M. (2000) *Advanced Drug Delivery Reviews*, **45**, 47–56.
- 5 Schröder, V. and Schubert, H. (1999) *Colloid and Surfaces*, **152** (1), 103–109.
- 6 Joscelyne, S.M. and Trägårdh, G. (2000) *Journal of Membrane Science*, **169**, 107–117.
- 7 Charcosset, C., Limayem, I. and Fessi, H. (2004) *Journal of Chemical Technology and Biotechnology*, **79**, 209–218.
- 8 Abrahamse, A.J., van der Padt, A. and Boom, R.M. (2004) *Journal of Membrane Science*, **230**, 149–159.
- 9 Vladislavljević G.T. and Williams, R.A. (2005) *Advances in Colloid Interface Science*, **113**, 1–20.
- 10 Lambrich, U. and Schubert, H. (2005) *Journal of Membrane Science*, **257**, 76–84.
- 11 Suzuki, K., Shuto, I. and Hagura, Y. (1996) *Food Science and Technology International Tokyo*, **2** (1), 43–47.
- 12 Kawakatsu, T., Kikuchi, Y. and Nakajima, M. (1997) *Journal of the American Oil Chemists Society*, **74**, 317–321.
- 13 Peng, S.J. and Williams, R.A. (1998) *Transactions of IChemE*, **76**, 894–901.
- 14 Vladislavljević G.T., Tesch, S. and Schubert, H. (2002) *Chemical Engineering and Processing*, **41**, 231–238.
- 15 Vladislavljević G.T., Shimizu, M. and Nakashima, T. (2004) *Journal of Membrane Science*, **244** (1–2), 97–106.
- 16 Vladislavljević G.T. and Schubert, H. (2003) *Journal of Membrane Science*, **223**, 15–23.
- 17 Christov, N.C., Danov, K.D., Danova, D.K. and Kralchevsky, P.A. (2008) *Langmuir*, **24**, 1397–1410.
- 18 van der Graaf, S., Nisisako, T., Schröen, C.G.P.H., van der Sman, R.G.M. and Boom, R.M. (2006) *Langmuir*, **22**, 4144–4152.
- 19 Cheng, C.J., Chu, L.Y. and Xie, R. (2006) *Journal of Colloids and Interface Science*, **300**, 375–382.
- 20 Sotoyama, K., Asano, Y., Ihara, K., Takahashi, K. and Doi, K. (1999) *Journal of Food Science*, **64** (2), 221–215.
- 21 Vladislavljević G.T., Kobayashi, I., Nakajima, M., Williams, R.A., Shimizu, M. and Nakashima, T. (2007) *Journal of Membrane Science*, **302**, 243–253.
- 22 Scherze, I., Marzilger, K. and Muschiolik, G. (1999) *Colloids and Surface B*, **12**, 213–221.
- 23 Mine, Y., Shimizu, M. and Nakashima, T. (1996) *Colloids and Surfaces B: Biointerfaces*, **6** (4), 261–268.
- 24 Fuchigami, T., Toki, M. and Nakanishi, K. (2000) *Journal of Sol-Gel Science and Technology*, **19**, 337–341.
- 25 Wu, J., Jing, W., Xing, W. and Xu, N. (2006) *Desalination*, **193**, 381–386.
- 26 Schröder, V., Behrend, O. and Schubert, H. (1998) *Journal of Colloid and Interface Science*, **202**, 334–340.
- 27 Joscelyne, S.M. and Trägårdh, G. (1999) *Journal of Food Engineering*, **39**, 59–64.
- 28 Berot, S., Giraudet, S., Riaublanc, A., Anton, M. and Popineau, Y. (2003) *Transactions of IChemE*, **81**, 1077–1082.
- 29 Giorno, L., Mazzei, R., Oriolo, M., De Luca, G., Davoli, M. and Drioli, E. (2005) *Journal of Colloid and Interface Science*, **287**, 612–623.
- 30 Yamazaki, N., Yuyama, H., Nagai, M., Ma, G.H. and Omi, S. (2002) *Journal of Dispersion Science and Technology*, **23** (1–3), 279–292.
- 31 Kobayashi, I., Yasuno, M., Iwamoto, S., Shono, A., Satoh, K. and Nakajima, M.

- (2002) *Colloids and Surface A*, **207**, 185–196.
- 32 Shima, M., Kobayashi, Y., Fujii, T., Tanaka, M., Kimura, Y., Adachi, S. and Matsuno, R. (2004) *Food Hydrocolloids*, **18** (1), 61–70.
- 33 Correia, L.A., Pex, P.A.C., van der Padt, A. and Poortinga, A.T. (2004) Presented at 8th International Conference on Inorganic Membrane (ICIM 9), 2004, Cincinnati, USA, 18–22 July.
- 34 Park, S., Yamaguchi, T. and Nakao, S. (2001) *Chemical Engineering Science*, **56** (11), 3539–3548.
- 35 Shima, M., Kobayashi, Y., Fujii, T., Tanaka, M., Kimura, Y., Adachi, S. and Matsuno, R. (2004) *Food Hydrocolloids*, **18**, 61–70.
- 36 Ribeiro, H.S., Rico, L.G., Badolato, G.G. and Schubert, H. (2005) *Journal of Food Science*, **70** (2), E117–E123.
- 37 Kondo, A. (1979) History and classification of microencapsulation, in *Microcapsule Processing and Technology* (ed. J. Wade Van Valkenburg), Marcel Dekker, New York, NY, Chapter 4.
- 38 Thies, C. (1996) A survey of microencapsulation processes, in *Microencapsulation Methods and Industrial Applications* (ed. S. Benita), vol. 17, Marcel Dekker, New York, pp. 1–21.
- 39 Wang, Z., Wang, S., Volker, S. and Schubert, H. (2000) *Chinese Journal of Chemical Engineering*, **8**, 108–112.
- 40 Danov, K.D., Danova, D.K. and Kralchevsky, P.A. (2007) *Journal of Colloid and Interface Science*, **316**(2), 844–857.
- 41 O'Neil, M.E. (1964) *Mathematika*, **11**, 67–74.
- 42 Ken, H.J. and Chen, P.Y. (2001) *Chemical Engineering Science*, **56**, 6863–6871.
- 43 Kosvintsev, S.R., Gasparini, G., Holdich, R.G., Cumming, I.W. and Stillwell, M.T. (2005) *Industrial & Engineering Chemistry Research*, **44**, 9323–9330.
- 44 Kelder, J.D.H., Janssen, J.J.M. and Boom, R.M. (2007) *Journal of Membrane Science*, **304**, 50–59.
- 45 Chatterjee, J. (2002) *Advances in Colloid Interface Science*, **98**, 265–283.
- 46 De Luca, G. and Drioli, E. (2006) *Journal of Colloid and Interface Science*, **294**, 436–448.
- 47 De Luca, G., Di Maio, F.P., Di Renzo, A. and Drioli, E. (2008) *Chemical Engineering and Processing*, **47**, 1150–1158.
- 48 Xu, J.H., Luo, G.S., Chen, G.G. and Wang, J.D. (2005) *Journal of Membrane Science*, **266**, 121–131.
- 49 van Rijn, C.J.M. (2000) *Nano and Micro Engineered Membrane Technology* in Membrane Science and Technology Series, vol. 10, Amsterdam, Elsevier.
- 50 De Luca, G., Sindona, A., Giorno, L. and Drioli, E. (2004) *Journal of Membrane Science*, **229**, 199–209.
- 51 van der Graaf, S., Schröen, C.G.P.H., van der Sman, R.G.M. and Boom, R.M. (2004) *Journal of Colloid and Interface Science*, **277**, 456–463.
- 52 Rayner, M., Trägårdh, G., Trägårdh, C. and Dejmeek, P. (2004) *Journal of Colloid and Interface Science*, **279**, 175–185.
- 53 Rayner, M., Trägårdh, G. and Trägårdh, C. (2005) *Colloids and Surface A: Physicochemical and Engineering, Aspects* **266**, 1–17.
- 54 Ohta, M., Yamamoto, M. and Suzuki, M.M. (1995) *Chemical Engineering Science*, **50**, 2923–2931.
- 55 Abrahamse, A.J., van der Padt, A., Boom, R.M. and de Heij, W.B.C. (2001) *AIChE Journal*, **47** (6), 1285–1291.
- 56 Kobayashi, I., Mukataka, S. and Nakajima, M. (2004) *Langmuir*, **20**, 9868–9875.
- 57 Cristini, V. and Tan, Y.-C. (2004) *Lab on a Chip*, **4** (257), 257–264.
- 58 Kalarakis, A.N., Burganos, V.N. and Payatakes, A.C. (2003) *Physical Review E*, **67**, 016702-1–016702-8.
- 59 Okonogi, S., Kato, R., Asano, Y., Yuguchi, H., Kumazawa, R., Sotoyama, K., Takahashi, K. and Fujimoto, M. (1994) US5279847.
- 60 Okonogi, S., Kumazawa, R., Toyama, K., Kato, M., Asano, Y., Takahashi, K. and Fujimoto, M. (1992) JP4258251.
- 61 van der Graaf, S., Schröen, C.G.P.H. and Boom, R.M. (2005) *Journal of Membrane Science*, **251**, 7–15.

- 62 Gaonkar, A.G. (1994) US 5332595.
- 63 Higashi, S., Shimizu, M. and Setoguchi, T. (1996) *Colloids and Surface B*, **6**, 261–268.
- 64 Higashi, S., Shimizu, M., Nakashima, T., Iwata, K., Uchiyaemotherapyma, F., Tateno, S., Tamura, S. and Setoguchi, T. (1995) *Cancer*, **75**, 1245–1254.
- 65 Higashi, S. and Setoguchi, T. (2000) *Advanced Drug Delivery Reviews*, **45**, 57–64.
- 66 Guanghui, M., Hui, S., Zhiguo, S. and Lianyan, W. (2005) CN1600295.
- 67 Nakajma, M., Nabetani, H., Ichikawa, S. and Xu, Q.Y. (2003) US6538019.
- 68 Vladislavljević, G.T., Shimizu, M. and Nakashima, T. (2006) *Journal of Membrane Science*, **284**, 373–383.
- 69 Liu, R., Ma, G.H., Wan, Y.H. and Su, Z.G. (2005) *Colloid and Surface B: Biointerfaces*, **45**, 144–153.
- 70 Ito, F. and Makino, K. (2004) *Colloid and Surface B: Biointerfaces*, **39**, 17–21.
- 71 Omi, S., Katami, K., Yamamoto, A. and Iso, M. (1994) *Journal of Applied Polymer Science*, **51**, 1–11.
- 72 Shiga, K., Muramatsu, N. and Kondo, T. (1996) *Journal of Pharmacy and Pharmacology*, **48**, 891–895.
- 73 Costa, M.S. and Cardoso, M.M. (2006) *Desalination*, **200**, 498–500.
- 74 Shiga, K., Muramatsu, N. and Kondo, T. (1996) *Journal of Pharmacy and Pharmacology*, **48**, 891–895.
- 75 Wang, L.Y., Ma, G.H. and Su, Z.G. (2005) *Journal of Controlled Release*, **106**, 62–75.
- 76 Wang, L.Y., Gu, Y.H., Zhou, O.Z., Ma, G.H., Wan, Y.H. and Su, Z.G. (2006) *Colloid and Surface B: Biointerfaces*, **50**, 126–135.
- 77 Fuchigami, T., Toki, M. and Nakanishi, K. (2000) *Journal of Sol-Gel Science and Technology*, **19**, 337–341.
- 78 Nagashima, S., Koide, M., Ando, S., Makino, K., Tsukamoto, T. and Ohshima, T. (1999) *Colloids and Surfaces A: Physicochemical and Engineering Aspects*, **153**, 221–227.
- 79 Makino, K., Agata, H. and Ohshima, H. (2000) *Journal of Colloid and Interface Science*, **230**, 128–134.
- 80 Charcosset, C., El-Harati, A. and Fessi, H. (2005) *Journal of Controlled Release*, **108**, 112–120.
- 81 Dowding, P.J., Goodwin, J.W. and Vincent, B. (2001) *Colloids and Surfaces A: Physicochemical and Engineering Aspects*, **180**, 301–309.
- 82 Omi, S., Matsuda, A., Imamura, K., Nagai, M. and Ma, G.H. (1999) *Colloids and Surface A: Physicochemical and Engineering Aspects*, **153**, 373–381.
- 83 Ma, G.H., Su, G.Z., Omi, S., Sundberg, D. and Stubbs, J. (2003) *Journal of Colloid and Interface Science*, **266**, 282–294.
- 84 Ma, G.H., Nagai, M. and Omi, S. (1999) *Journal of Colloid and Interface Science*, **214**, 264–282.
- 85 Ma, G.H., Nagai, M. and Omi, S. (1999) *Colloids Surfaces A: Physicochemical and Engineering Aspects*, **153**, 383–394.
- 86 Muramatsu, N. and Kondo, T. (1995) *Journal of Microencapsulation*, **12**, 129–136.
- 87 Roulier, V. and Quemain, E. (2000) WO0021491.
- 88 Giorno, L., Piacentini, E., Mazzei, R. and Drioli, E. *Journal of Membrane Science*, **317** (1–2), 19–25.
- 89 Kiyoshi, E. (1999) JP11242317.
- 90 Aryanti, N., Williams, R.A., Hou, R. and Vladislavljević, G.T. (2006) *Desalination*, **200**, 572–574.
- 91 Yuyama, H., Yamamoto, K., Shirafuji, K., Nagai, M., Ma, G.H. and Omi, S. (2000) *Journal of Applied Polymer Science*, **77**, 2237–2245.
- 92 Ma, G.H., An, C.J., Yuyama, H., Su, Z.G. and Omi, S. (2003) *Journal of Applied Polymer Science*, **89**, 163–178.
- 93 Ha, Y.K., Song, H.S., Lee, H.J. and Kim, J.H. (1999) *Colloids and Surface A: Physicochemical and Engineering Aspects*, **162**, 289–293.
- 94 Ha, Y.K., Song, H.S., Lee, H.J. and Kim, J.H. (1998) *Colloids and Surface A: Physicochemical and Engineering Aspects*, **145**, 281–284.
- 95 Westover, D., Seitz, W.R. and Lavine, B.K. (2003) *Microchemical Journal*, **74**, 121–129.

- 96** Figoli, A., De Luca, G., Lamerata, F. and Drioli, E. (2006) *Desalination*, **199**, 115–117.
- 97** Figoli, A., De Luca, G., Longavita, E. and Drioli, E. (2007) *Separation Science and Technology*, **42**, 2809–2827.
- 98** Figoli, A., De Luca, G. and Drioli, E. (2007) *Italian Journal of Food Science*, ISSN 1120-1770, **XI**, 90–96.
- 99** Nakajima, N., Fujiwara, M., Maeda, D. and Watanabe, K. (2006) JP2006182890.